

Unified Generation-Refinement Planning: Bridging Guided Flow Matching and Sampling-Based MPC for Social Navigation

Kazuki Mizuta¹ and Karen Leung^{1,2}

Abstract—Planning safe and effective robot behavior in dynamic, human-centric environments remains a core challenge due to the need to handle multimodal uncertainty, adapt in real-time, and ensure safety. Optimization-based planners offer explicit constraint handling but performance relies on initialization quality. Learning-based planners better capture multimodal possible solutions but struggle to enforce constraints such as safety. In this paper, we introduce a unified generation-refinement framework bridging learning and optimization with a novel *reward-guided conditional flow matching* (CFM) model and model predictive path integral (MPPI) control. Our key innovation is in the incorporation of a *bidirectional information exchange*: samples from a reward-guided CFM model provide informed priors for MPPI refinement, while the optimal trajectory from MPPI warm-starts the next CFM generation. Using autonomous social navigation as a motivating application, we demonstrate that our approach can flexibly adapt to dynamic environments to satisfy safety requirements in real-time.

I. INTRODUCTION

Robust planning in dynamic human-centric environments (e.g., warehouses, sidewalks, airports) requires fast replanning, safety constraint enforcement, and reasoning over uncertain, multimodal human behavior [1], [2], [3], [4]. Optimization- and learning-based methods have shown strong performance in settings like human-robot interaction [4], [5], mobile autonomy [6], [7], and manipulation [8], but struggle to meet all demands simultaneously. Optimization-based methods [9] offer real-time performance and constraint handling, yet falter in dynamic, uncertain environments [10]. Learning-based approaches (e.g., diffusion policies [11], [12], [13]) are well adept at handling multimodal uncertainty but lack constraint guarantees and are often slow at inference. Naturally, leveraging learning-based methods as trajectory priors in optimization-based planners offers a compelling path forward, but real-world deployment still hinges on computational efficiency and reliable constraint satisfaction.

Conditional flow matching (CFM) models [14] have emerged as a promising learning-based solution, achieving generation quality comparable to that of diffusion models while significantly reducing inference time. CFMs have demonstrated success in robotic applications [15], [16], but their application to safety-critical tasks in dynamic environments that require meeting constraints in real-time remains underexplored. To address this, we propose a framework that combines guided CFM with online optimization-based planning: CFM offers multimodal trajectory candidates, while optimization enforces constraint satisfaction and responsiveness

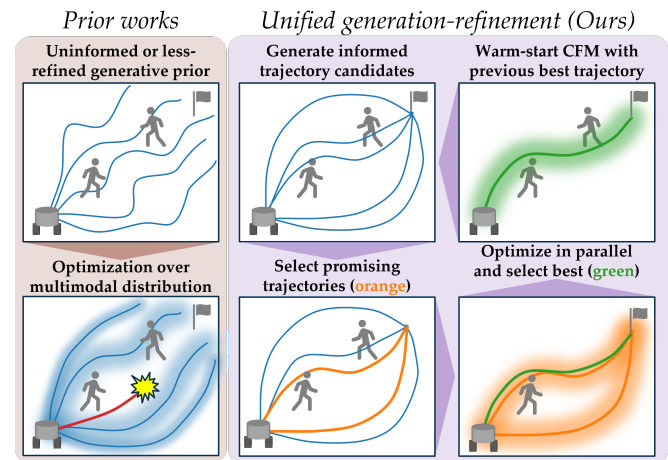


Fig. 1: Overview of the proposed unified planning framework for dynamic environments: At each planning step, our conditional flow matching (CFM) model generates context-aware and multimodal trajectory candidates guided by a reward function. Promising candidates are selected, then refined, and the best trajectory is selected and executed. The optimal trajectory warm-starts the next CFM generation for the next planning step.

to dynamic environments. Illustrated in Fig. 1, we introduce a safety-guided CFM model to produce informed priors for sampling-based MPC, specifically model predictive path integral (MPPI) control [6]. We then select the most promising trajectory candidates, allowing MPPI to refine each selected candidate in parallel, and then select the best one. The MPC output then warm-starts the next CFM step, creating a bidirectional feedback loop that improves efficiency and performance. We validate our approach in a social navigation task, where a robot must safely and efficiently navigate through crowds of moving humans. Our method enables real-time adaptation to uncertain human behavior, achieving the safest behavior without significantly compromising on goal-reaching or control smoothness.

Statement of contributions. Our contributions are fourfold: **(i)** A novel planning framework that synergistically integrates CFM with MPPI, combining CFM’s generative expressiveness with MPPI’s optimization efficiency. **(ii)** A reward-guided CFM sampling mechanism that adapts trajectories to new planning objectives at test time without retraining. **(iii)** A mode-selective MPPI that utilizes the multimodal trajectories generated by CFM, enabling refinement of these paths without collapsing distinct modes into a suboptimal solution. **(iv)** Evaluation on social navigation tasks, demonstrating significant improvements over standalone approaches in terms of solution quality, safety, and generation time.

Kazuki Mizuta is partially supported by the Nakajima Foundation.

¹University of Washington, Department of Aeronautics and Astronautics,
² NVIDIA, Contact: {mizuta, kymleung}@uw.edu

II. RELATED WORK

This section reviews relevant prior work in optimization-based trajectory planning approaches and recent advances in data-driven generative models for motion planning.

Learned initializations for optimization-based trajectory planning. Optimization-based methods are well-suited for safety-critical trajectory planning due to their fast computation and explicit constraint handling. However, they rely on accurate system models and require good initializations to ensure convergence to high-quality solutions. Common initialization strategies, such as straight-line trajectories, previous solutions, or Gaussian sampling, are simple but unimodal, thus limiting performance in non-convex settings like dynamic obstacle avoidance. Recent work addresses this by learning informed initializations or sampling distributions conditioned on the environment [17], [18], [19], [20], [21], [22], [23]. While effective, these approaches often require (near-)optimal demonstrations for training, struggle to scale in multi-agent dynamic settings, and generalize poorly to out-of-distribution environments.

Recent work improves online responsiveness by biasing sampling distributions with explicitly computed backup policies (e.g., contingency plans) [24], [25]. While effective, these methods require solving additional planning problems, incorporating system-specific knowledge, or relying on handcrafted heuristics—adding computational overhead, and limiting generalization. In contrast, we propose learning a sampling distribution from real-world data and introducing a lightweight, flexible guidance mechanism to bias sampling online with minimal cost and without additional training.

Diffusion policies. Deep generative models have shown strong performance in learning complex distributions [26], [27]. Guided diffusion models [11], [12], [28] are popular due to their stability, expressivity, and ability to incorporate reward-based guidance, making them effective for planning and trajectory generation tasks [8], [13], [29], [30], [31], [32]. However, they face two key limitations: (i) high computational cost from iterative denoising, and (ii) limited ability to enforce constraints, as rewards guide but do not guarantee constraint satisfaction. These drawbacks hinder their use in real-time, safety-critical control.

Conditional flow matching. Conditional flow matching (CFM) models [14] offer a promising alternative to diffusion models, achieving comparable generation quality while significantly reducing inference time by learning a direct mapping from noise to data, thereby avoiding iterative denoising. This efficiency makes CFMs better suited for real-time control [15], [16]. While classifier-free guidance, initially developed for diffusion models [28], has been adapted for CFMs [33], it requires labeled data, which is often unavailable. Alternatively, classifier-based reward guidance can bias generation during inference without labels [13]. Our work explores this latter direction, developing a novel safety-guided CFM that leverages control barrier functions to generate constraint-aware trajectories for robot navigation.

III. PRELIMINARIES: CONDITIONAL FLOW MATCHING

Conditional flow matching (CFM) [14] is a simulation-free method for training continuous normalizing flows [34] that transforms a simple source distribution p into a target data distribution q . Given a data point $\mathbf{z}_1 \sim q(\mathbf{z}_1 | \mathbf{c}) \in \mathbb{R}^{d_z}$ with condition $\mathbf{c} \in \mathbb{R}^{d_c}$, and a sample from source distribution $\mathbf{z}_0 \sim p(\mathbf{z}_0)$, let $p(\mathbf{z}_0) = \mathcal{N}(0, I)$, CFM learns a velocity field $v : \mathbb{R}^{d_z} \times \mathbb{R}^{d_c} \times [0, 1] \rightarrow \mathbb{R}^{d_z}$ that defines an ODE $\frac{d\mathbf{z}_\tau}{d\tau} = v_\theta(\mathbf{z}_\tau, \mathbf{c}, \tau)$. To avoid confusion with physical time, we use $\tau \in [0, 1]$ to denote the flow time parameter. Solving this ODE from $\tau = 0$ to $\tau = 1$ maps a sample from the source distribution to a sample from the target distribution $q(\mathbf{z}_1 | \mathbf{c})$. A key idea in CFM is defining a probability path $p_\tau(\mathbf{z} | \mathbf{c})$ that smoothly interpolates between the source distribution at $\tau = 0$ and the target data distribution at $\tau = 1$:

$$p_\tau(\mathbf{z} | \mathbf{c}) = \int p_{\tau|1}(\mathbf{z} | \mathbf{z}_1)q(\mathbf{z}_1 | \mathbf{c})d\mathbf{z}_1, \quad (1)$$

where $p_{\tau|1}(\mathbf{z} | \mathbf{z}_1) = \mathcal{N}(\tau\mathbf{z}_1, (1 - \tau)^2 I)$.

During training, we sample a flow time $\tau \sim U(0, 1)$, data points $\mathbf{z}_1 \sim q(\mathbf{z}_1 | \mathbf{c})$, and noise $\mathbf{z}_0 \sim p(\mathbf{z}_0)$. Considering velocity fields conditioned on \mathbf{z}_1 to generate conditional probability paths, an intermediate point $\mathbf{z}_\tau = (1 - \tau)\mathbf{z}_0 + \tau\mathbf{z}_1$ has time derivative $\dot{\mathbf{z}}_\tau = \mathbf{z}_1 - \mathbf{z}_0$. Therefore, to learn a CFM, the velocity field is parameterized as a neural network v_θ and optimize using the following CFM loss function,

$$L_{\text{CFM}} = \mathbb{E}_{\tau, q(\mathbf{z}_1 | \mathbf{c}), p(\mathbf{z}_0)} [\|\mathbf{v}_\theta(\mathbf{z}_\tau, \mathbf{c}, \tau) - (\mathbf{z}_1 - \mathbf{z}_0)\|_2^2]. \quad (2)$$

During inference, we sample $\mathbf{z}_0 \sim p(\mathbf{z}_0)$ and solve the ODE with the learned velocity field v_θ from $\tau = 0$ to $\tau = 1$ to generate samples from the conditional distribution $q(\mathbf{z}_1 | \mathbf{c})$.

IV. PROBLEM FORMULATION

This work addresses the challenge of generating safe, efficient, and socially-aware trajectories for a robot navigating through dynamic environments populated by humans. We formulate this as a finite-horizon optimal control problem. Our goal is to compute a sequence of control inputs for the robot that minimizes a given cost function while satisfying system dynamics and safety constraints.

Let a robot state trajectory be denoted as $\mathbf{x} = [\mathbf{x}_0, \dots, \mathbf{x}_{T+1}]$ where $\mathbf{x}_t \in \mathcal{D} \subseteq \mathbb{R}^{d_x}$ and control inputs as $\mathbf{u} = [\mathbf{u}_1, \dots, \mathbf{u}_T]$ where $\mathbf{u}_t \in \mathcal{U} \subseteq \mathbb{R}^{d_u}$, where T represents the planning horizon. The robot's motion is governed by a discrete-time dynamics model $\mathbf{x}_{t+1} = f(\mathbf{x}_t, \mathbf{u}_t)$ where f represents the robot's dynamics function. The environment contains a set of N dynamic human agents. The state of the i -th human at time t is denoted by $\mathbf{x}_{h_i, t}$.

The planning problem is to find an optimal control sequence \mathbf{u} that minimizes a cost function $J(\mathbf{x}, \mathbf{u})$, which encapsulates performance criteria such as goal-reaching and control smoothness. A critical requirement for this problem is ensuring the robot's safety. We define safety as maintaining a minimum separation distance r_{safe} from all human agents at all times. This is expressed as a hard constraint for all

$t \in [0, T]$ and for all humans $i \in \{1, \dots, N\}$,

$$\|\mathbf{p}_t - \mathbf{p}_{h_i,t}\|_2 \geq r_{\text{safe}}, \quad (3)$$

where \mathbf{p}_t and $\mathbf{p}_{h_i,t}$ are the positions of the robot and the i -th human at time t , respectively. In summary, the planning problem can be formally stated as

$$\begin{aligned} \min_{\mathbf{u}} \quad & J(\mathbf{x}, \mathbf{u}) \\ \text{s.t.} \quad & \mathbf{x}_{t+1} = f(\mathbf{x}_t, \mathbf{u}_t), \mathbf{x}_0 = \mathbf{x}_{\text{init}}, t = 1, \dots, T-1 \\ & \|\mathbf{p}_t - \mathbf{p}_{h_i,t}\|_2 \geq r_{\text{safe}}, i = 1, \dots, N, t = 0, \dots, T \\ & \mathbf{u}_t \in \mathcal{U}, t = 0, \dots, T-1. \end{aligned} \quad (4)$$

The challenge lies in solving this optimization problem in real-time within complex, uncertain, and multimodal environments, where human motions are not known in advance. Our proposed framework aims to address this by combining the strengths of a generative model for creating diverse, prospective trajectory candidates and an optimization-based controller for refining these trajectories to ensure safety and task performance.

V. GUIDED CONDITIONAL FLOW MATCHING FOR TRAJECTORY OPTIMIZATION

Our goal is to develop a planning framework for autonomous robots in complex, dynamic environments. We combine conditional flow matching (CFM) with sampling-based model predictive control (MPC) to enable real-time adaptation to environmental changes. In this section, we discuss how we can guide a CFM model to generate informed trajectory candidates to improve MPC solution quality.

A. CFM model training

In this work, we use a CFM model to transform random noise into a realistic control sequence \mathbf{u} . As such, we have \mathbf{z} from the CFM definition from Sec. III corresponds to \mathbf{u} . Specifically, the target distribution consists of control sequences from pedestrian trajectory data and is conditioned on \mathbf{c} , the robot's current state, goal position, and previously executed controls.

Training loss. The CFM loss L_{CFM} (2) ensures that our model learns a velocity field that transforms noise into realistic control sequences but does not explicitly enforce the task objective of reaching a goal. To make the training more efficient and directly encourage goal-directed behavior, we augment the learning objective with goal loss L_{goal} .

To compute the goal loss, we first generate a control sequence $\mathbf{u} = \mathbf{z}_1$ and apply it to the robot's dynamics to predict the resulting state sequence \mathbf{x} . We then measure the squared Euclidean distance between the trajectory's final position \mathbf{p}_T and the goal position \mathbf{p}_{goal} . The final training loss is a weighted sum of these two components:

$$L = L_{\text{CFM}} + \lambda_{\text{goal}} L_{\text{goal}}, \quad (5)$$

where $L_{\text{goal}} = \|\mathbf{p}_{\text{goal}} - \mathbf{p}_T\|^2$ and λ_{goal} is a hyperparameter describing the importance of the goal loss.

Conditioning on past controls. To ensure that generated trajectories are fluent, we also input previously executed actions to discourage abrupt changes in motion. To achieve this, we

design the condition \mathbf{c} to include a history of past controls. Rather than considering only the current environment and goals at each planning step, we incorporate the history of past control actions by inpainting during data generation. The length of control history presents an important trade-off: longer histories produce smoother control sequences with better continuity from previous actions, but may reduce responsiveness to dynamic changes in the environment. This historical conditioning mechanism enables our model to generate control sequences that maintain temporal coherence.

We can train a CFM model using the loss function and conditioning information, and this will produce a velocity field v_{θ} . Next, we describe how we can augment the velocity field with a user-provided reward function without the need for training, thus enabling flexible behavior synthesis online.

B. CFM guidance with reward functions

To steer the generation process towards trajectories with desirable properties, we incorporate reward-based guidance into the CFM trajectory generation process. Inspired by classifier-guided diffusion models with reward functions [13], we adapt this concept to the flow matching framework. First, we present how the velocity field is adapted to handle user-specified rewards, and describe how to generate samples using the CFM model guided by the reward.

Proposition 1 (Reward-guided CFM Velocity Field):

Given a base velocity field $v_{\theta}(\mathbf{z}_{\tau}, \mathbf{c}, \tau)$ and a differentiable reward function $R(\mathbf{z}_1)$, the *guided* velocity field $\tilde{v}_{\theta}(\mathbf{z}_{\tau}, \mathbf{c}, \tau)$ is given by

$$\tilde{v}_{\theta}(\mathbf{z}_{\tau}, \mathbf{c}, \tau) = v_{\theta}(\mathbf{z}_{\tau}, \mathbf{c}, \tau) + \lambda_{\text{guide}} \nabla_{\mathbf{z}_1} R(\mathbf{z}_1), \quad (6)$$

where λ_{guide} is a hyperparameter controlling guidance strength.

Proof: Following the control-as-inference approach from [13], [35], let \mathbf{y} be a binary random variable representing where $\mathbf{y} = 1$ denotes *optimality*. Specifically, it is chosen that $p_{\tau}(\mathbf{y} = 1 \mid \mathbf{z}_1) = \exp(R(\mathbf{z}_1))$ where R is a reward function measuring the performance of a desired task. We drop the “= 1” in the remainder of the derivation for conciseness. Using [33, Lem. 1] on (1), we can apply Bayes' rule to the conditional velocity field $v_{\tau}(\mathbf{z}_{\tau} \mid \mathbf{y})$ and then group terms depending only on \mathbf{z}_{τ} ,

$$\begin{aligned} v_{\tau}(\mathbf{z}_{\tau} \mid \mathbf{y}) &= \frac{1}{\tau} \mathbf{z}_{\tau} + \frac{1-\tau}{\tau} \nabla_{\mathbf{z}_{\tau}} \log p_{\tau}(\mathbf{z}_{\tau} \mid \mathbf{y}), \quad ([33, \text{Lem. 1}]) \\ v_{\tau}(\mathbf{z}_{\tau} \mid \mathbf{y}) &= \frac{1}{\tau} \mathbf{z}_{\tau} + \frac{1-\tau}{\tau} \nabla_{\mathbf{z}_{\tau}} \log \left(\frac{p_{\tau}(\mathbf{y} \mid \mathbf{z}_{\tau}) p_{\tau}(\mathbf{z}_{\tau})}{p_{\tau}(\mathbf{y})} \right), \\ &= \frac{1}{\tau} \mathbf{z}_{\tau} + \frac{1-\tau}{\tau} (\nabla_{\mathbf{z}_{\tau}} \log p_{\tau}(\mathbf{z}_{\tau}) + \nabla_{\mathbf{z}_{\tau}} \log p_{\tau}(\mathbf{y} \mid \mathbf{z}_{\tau})) \\ &= v_{\tau}(\mathbf{z}_{\tau}) + \frac{1-\tau}{\tau} \nabla_{\mathbf{z}_{\tau}} \log p_{\tau}(\mathbf{y} \mid \mathbf{z}_{\tau}), \quad ([33, \text{Lem. 1}]) \end{aligned}$$

where $v_{\tau}(\mathbf{z}_{\tau})$ represents the unconditional velocity field. Given the relationship between intermediate and predicted states $\tau \mathbf{z}_1 = \mathbf{z}_{\tau} - (1-\tau) \mathbf{z}_0$, we use the chain rule to express the gradient term,

$$\begin{aligned} v_{\tau}(\mathbf{z}_{\tau} \mid \mathbf{y}) &= v_{\tau}(\mathbf{z}_{\tau}) + \frac{1-\tau}{\tau} (\nabla_{\mathbf{z}_{\tau}} \mathbf{z}_1)^T \nabla_{\mathbf{z}_1} \log p_{\tau}(\mathbf{y} \mid \mathbf{z}_1) \\ &= v_{\tau}(\mathbf{z}_{\tau}) + \frac{1-\tau}{\tau^2} \nabla_{\mathbf{z}_1} \log p_{\tau}(\mathbf{y} \mid \mathbf{z}_1). \end{aligned}$$

Then following from [13] where $p_\tau(\mathbf{y} \mid \mathbf{z}_1) = \exp(R(\mathbf{z}_1))$, we have $\log p_\tau(\mathbf{y} \mid \mathbf{z}_1) = R(\mathbf{z}_1)$ and we introduce λ_{guide} as a hyperparameter to tune the guidance strength, which incorporates the term $\frac{1-\tau}{\tau^2}$. As such, we result in (6). ■

Reward guidance steps. To steer this process with a reward function, we introduce a multi-step iterative refinement, as summarized in Algorithm 1. This addresses the challenge that the guidance term $R(\mathbf{z}_1)$ depends on the final trajectory \mathbf{z}_1 , which is unknown at intermediate stages of generation.

Given a user-defined ODE schedule $\{\tau_0, \dots, \tau_N\}$, at each step τ_i , we first form a temporary estimate of the final trajectory \mathbf{z}_1 by integrating the current *unconditioned* velocity field $v_\theta(\mathbf{z}_{\tau_i}, \mathbf{c}, \tau_i)$ from $\tau = \tau_i$ to $\tau = 1$ (Line 4). Using this estimated trajectory, we then evaluate the reward function $R(\mathbf{z}_1)$ and compute its gradient (Line 5). This gradient is added to the unconditioned velocity field to create a *guided velocity field*, as shown in (6) (Line 6). Finally, we use this new guided velocity field to take a single integration step from τ_i to the next point τ_{i+1} .

Guided CFM vs guided Diffusion. An advantage of CFMs over diffusion models is the efficiency of trajectory generation. Diffusion models require multiple denoising steps while CFM generates trajectories by integrating the velocity field from a current τ to $\tau = 1$ in a few, or even a single, step. Unlike guided diffusion models that evaluate rewards on noisy trajectories [36], our reward-guided CFM approach evaluates rewards on estimated noise-free trajectories.

Although this process is iterative, it retains a significant efficiency advantage over guided diffusion. The number of function evaluations is typically very small (e.g., 5-10 steps), which is fewer than the dozens of steps often required by guided diffusion models. This allows our approach to adapt to dynamic environments in real-time without retraining the base CFM, striking a practical balance between single-shot efficiency and guided control.

C. Reward function

The user provides a reward function to guide the generation process. In this work, we consider a reward function that is a weighted sum of multiple objectives, such as safety, task performance, and control smoothness. Given the priority in collision avoidance for the problem of social navigation, we describe our choice of collision avoidance reward.

For safety, we employ control barrier functions (CBFs) [37] to define a safety reward function over states and controls. Specifically, we consider a CBF reward $r_{\text{safe}}(\mathbf{x}, \mathbf{u})$ to be the degree of violation of the CBF inequality. The CBF reward r_{safe} is defined as,

$$r_{\text{safe}}(\mathbf{x}_t, \mathbf{u}_t) = \gamma_t \cdot \min\{0, \dot{h}(\mathbf{x}_t) + \alpha(h(\mathbf{x}_t))\}, \quad (7)$$

$$h(\mathbf{x}_t) = \|\mathbf{p}_t - \mathbf{p}_{\text{hi},t}\|^2 - r^2,$$

where $\dot{h}(\mathbf{x}_t)$ denotes the time derivative of $h(\mathbf{x}_t)$, α is a extended-class \mathcal{K} function that bounded the rate at which the system approaches the unsafe set, and γ_t is a markup term that promotes proactive collision avoidance earlier in the horizon rather than later [38]. Note that the CBF reward depends on both controls *and states*, but our CFM model

Algorithm 1 Reward-Guided CFM Trajectory Generation

Require: Conditioning variable \mathbf{c} , guidance strength λ_{guide} , ODE schedule $\{\tau_0, \dots, \tau_N\}$

- 1: Initialize: $\mathbf{z}_0 \sim \mathcal{N}(0, I)$
- 2: **for** $i = 0$ **to** $N - 1$ **do**
- 3: Compute velocity field: $v_\theta(\mathbf{z}_{\tau_i}, \mathbf{c}, \tau_i)$
- 4: Integrate \mathbf{z}_{τ_i} from $\tau = \tau_i$ to $\tau = 1$ to obtain \mathbf{z}_1
- 5: Compute gradient $g = \nabla_{\mathbf{z}_1} R(\mathbf{z}_1)$
- 6: $\tilde{v}_\theta \leftarrow v_\theta(\mathbf{z}_{\tau_i}, \mathbf{c}, \tau_i) + \lambda_{\text{guide}} g$ (See (6))
- 7: $\mathbf{z}_{\tau_{i+1}} \leftarrow \mathbf{z}_{\tau_i} + \tilde{v}_\theta(\tau_{i+1} - \tau_i)$
- 8: **end for**
- 9: **return** \mathbf{z}_{τ_N}

only produces a control sequence and the reward gradient is taken with respect to controls. In evaluating the CBF reward, we integrate dynamics with the control sequence to obtain states, and rely on automatic differentiation to compute the gradient of the reward with respect to controls.

In addition to safety, other reward terms can be incorporated to influence different aspects of the behavior. The total reward function $R(\mathbf{u})$ with dynamics $\mathbf{x}_{t+1} = f(\mathbf{x}_t, \mathbf{u}_t)$ is a weighted sum over the planning horizon T ,

$$R(\mathbf{u}) = \sum_{t=0}^{T-1} w_{\text{safe}} r_{\text{safe}}(\mathbf{x}_t, \mathbf{u}_t) + w_o r_o(\mathbf{x}_t, \mathbf{u}_t), \quad (8)$$

where w_{safe} and w_o are scalar weights that balance the contribution of each component. The specific formulations for any additional reward components r_o and the weights w_o used in our experiments are detailed in Section VII.

VI. BRIDGING FLOW MATCHING WITH TRAJECTORY OPTIMIZATION

We propose using samples generated from our guided CFM model to inform a sampling-based MPC framework, and also using optimized trajectories from MPC to warm-start the guided CFM generation for the next planning step. In this paper, we specifically utilize model predictive path integral (MPPI) control [6], referring to our approach as **CFM-MPPI**, but our framework can be applied to other sampling-based MPC techniques. Fig. 2 illustrates the information flow between the CFM and MPC modules: CFM provides informative trajectory priors to MPC, and in return, the MPC solution warm-starts the next CFM generation, creating a synergistic feedback loop.

A. Benefits of integrating CFM with MPPI

While guided CFM generates trajectories conditioned by a reward function to satisfy certain constraints, it does not guarantee constraint satisfaction. This motivates the use of an optimization step to refine the trajectories, encouraging adherence to all required constraints. Furthermore, instead of having the CFM generate only a single trajectory, allowing it to produce multiple candidates and passing them to an optimization framework offers better search over a non-convex optimization landscape.

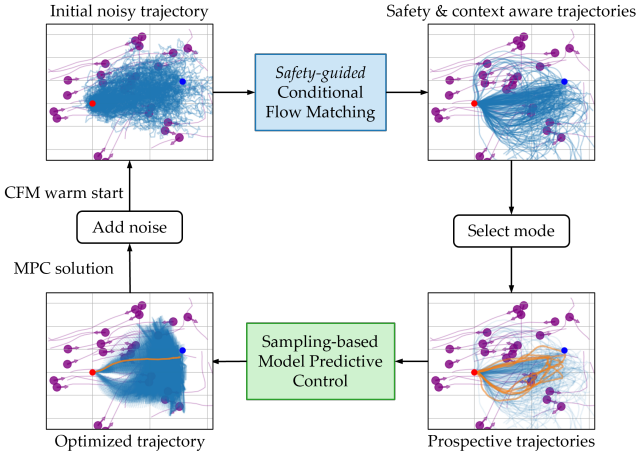


Fig. 2: A safety-guided conditional flow matching (CFM) model generates diverse trajectories as priors for model predictive control (MPC), which in turn warm-starts the next CFM sampling step.

Another key advantage is its adaptability to arbitrary robot dynamics, as the dynamics from the dataset may differ from those of the target deployment system. While the control commands from the CFM could be directly mapped to a different robot's dynamics, constraints imposed by the new dynamics could render the original trajectory suboptimal. Our framework refines the trajectory to bring it closer to an optimal solution under the specific dynamic constraints of the robot.

B. Mode selection: Handling multimodal priors from CFM

Unlike typical MPPI, which applies simple Gaussian perturbations to an initial trajectory, our approach leverages multiple trajectory candidates $\{\mathbf{u}_k\}_{k=1}^K$ sampled directly from our guided CFM model. These trajectories serve as samples from a prior distribution that encodes human-like motion patterns with added safety and goal-reaching considerations.

A key challenge arises when using trajectories generated by CFM as samples from a prior distribution for MPPI. Standard MPPI is designed to optimize a unimodal distribution of trajectories perturbed by Gaussian noise, calculating a cost-weighted average to find the optimal control. However, the distribution of trajectories generated by CFM can be multimodal. If a simple weighted average is computed across multiple distinct modes, the resulting trajectory could fall into an unfeasible or undesirable region between the modes, leading to optimization failure.

To address this issue, our approach first evaluates all trajectory candidates generated by the CFM and selects the K^* trajectories with the lowest cost. The selected trajectories then serve as the central paths for the standard MPPI algorithm. We then perturb each trajectory with Gaussian noise and execute the MPPI optimization to refine them in parallel. The trajectory with the lowest cost among the refined ones is selected as the output. Our approach of pre-selecting promising modes and then running independent MPPI optimizations for each one circumvents the problem of averaging across multiple distinct modes, which can force the resulting path into an suboptimal region.

C. Warmstarting CFM with MPC solutions

While the previous section focused on how the MPC framework utilizes trajectories generated by CFM, we now introduce a complementary mechanism for the reverse information flow: leveraging the optimized MPC solution to inform the next CFM generation. This establishes a bidirectional information loop between the generative model and the optimization framework, creating a synergistic relationship where each component progressively enhances the performance of the other.

We use the optimal control sequence from the previous MPC step to warm-start the CFM generation for the current step. Instead of sampling from the source distribution, we take the optimal control sequence from the previous step $\mathbf{u} = \mathbf{z}_1$ and perturb it with a controlled amount of Gaussian noise to create an intermediate latent variable \mathbf{z}_τ . The generative process then proceeds from this informed starting point.

This warm-starting strategy introduces a crucial trade-off that is governed by the magnitude of the injected noise. A small amount of noise biases the generator to produce trajectories that are highly consistent with the previous optimal path, promoting smooth and predictable behavior. Conversely, a larger amount of noise allows the generator to explore a more diverse set of trajectories, increasing its ability to discover novel solutions in response to significant changes in the environment. This mechanism not only accelerates convergence but also ensures that the generated trajectories maintain a logical continuity with past actions, which is essential for stable real-time control.

VII. EXPERIMENTS AND DISCUSSION

We evaluate the effectiveness of the proposed algorithm for social navigation tasks of an unicycle robot in dynamic human environments.

A. Experimental setup

Train and test data. We used the ETH pedestrian dataset [39] to train the CFM model. The dataset consists of 276,874 trajectories between 1 to 8 seconds long. The CFM represents pedestrians using single integrator dynamics, which we map to control inputs for the unicycle dynamics using the robot orientation and a control point offset. The linear velocity is the projection of the input velocity onto the robot's heading, while the angular velocity is derived to make the control point follow the path. For testing, we use the UCY pedestrian dataset [40], the SDD dataset [41], which contains faster-moving agents such as bicyclists, and a simulated crowd environment with 20 agents modeled by social force models (SFMs) [42]. We evaluate on 300 test scenarios for each. At each time step, it is generally assumed that the robot has access to the exact positions and velocities of all obstacles, and it predicts their future trajectories under a constant velocity assumption. For the SFM simulations, we also evaluated robustness to noisy observations by perturbing obstacle positions and velocities with Gaussian noise with standard deviation set to 0.02 and 0.2, respectively.

CFM model details. We use a transformer model [43] as the backbone of the CFM handling arbitrary trajectory length. We set $\lambda_{\text{goal}} = 0.1$ from (5). For the initial reward-guided trajectory generation, we use a 9-step ODE schedule: [0.0, 0.5, 0.8, 0.85, 0.9, 0.92, 0.94, 0.96, 0.98, 1.00]. For subsequent steps, the generation is warm-started at $\tau = 0.8$ using the previous MPPI solution, reducing the process to the final 7 steps. For the reward function, we set guidance strength $\lambda_{\text{guide}} = 1.0$, $w_{\text{goal}} = 0.1$, markup factor to 1.01, and to generate diverse trajectories spanning conservative and aggressive trajectories, we use five different values $w_{\text{safe}} = [0.1, 0.3, 0.5, 0.7, 0.9]$ for the safety reward and generate 40 trajectories for each value, totaling 200 trajectories. We set a collision radius of $r_{\text{safe}} = 0.5\text{m}$.

Guided CFM reward functions. The reward function $R(\mathbf{u})$ used for CFM guidance is composed of the CBF-based safety reward r_{safe} along with a goal reward which incentivizes the agent to reach its designated target \mathbf{x}_g based on the negative squared Euclidean distance at the final timestep T .

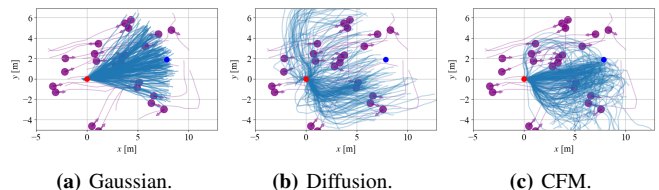
Cost functions for MPPI. The structure of this cost function is conceptually the inverse of the reward function and it similarly comprises components for safe, goal-reaching, and motion smoothness. For the safety cost c_{safe} , instead of using a CBF-based penalty, for the MPPI implementation, we define a safety cost that penalizes proximity to obstacles using an exponential function:

$$c_{\text{safe}}(\mathbf{p}_t) = \exp(-\beta(\|\mathbf{p}_t - \mathbf{p}_{\text{hi},t}\|^2 - r^2)), \quad (9)$$

where β is a positive scaling factor that defines the steepness of the potential field. The smoothness cost c_{smooth} penalizes the squared difference between control inputs at consecutive timesteps, $c_{\text{smooth}}(\mathbf{u}_t, \mathbf{u}_{t-1}) = \|\mathbf{u}_t - \mathbf{u}_{t-1}\|^2$.

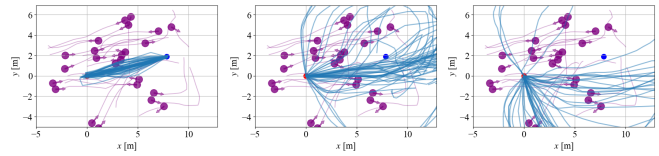
Comparison methods. We compare our method against the following methods. **MPPI**: A standard MPPI framework utilizing a Gaussian prior for the sampling distribution, where the initial trajectory consists of rotating to face the goal, then driving straight. **CFM**: Selecting the trajectory with the minimum cost among samples from the reward-guided CFM model. **Diff-MPPI**: A guided-diffusion model serving as a prior distribution for MPPI. **CFM-MPPI**: A guided CFM model serving as a prior distribution for MPPI. **Diff-MPPI***, **CFM-MPPI***: The asterisk * on CFM-MPPI and Diff-MPPI denotes the use of mode-selective MPPI, whereas the unmarked versions apply MPPI directly to the samples.

Our implementation of MPPI follows the algorithm in [6], with the following hyperparameter configuration: perturbation covariance $\sigma = [0.4, 0.2]$, temperature parameter $\lambda = 0.5$. For the backbone of the diffusion model, we employed the same transformer architecture as CFM. Like our CFM, the diffusion model was trained using a combination of a diffusion loss and a goal loss. To ensure our diffusion model’s computation time was competitive with that of a CFM (within 10Hz planning rate), we implemented a denoising diffusion implicit model (DDIM) for inference. Although the model was trained for 1000 denoising steps, we reduced this to 50 steps during inference, applying guidance only in the final 10 steps. During inference, the



(a) Gaussian. (b) Diffusion. (c) CFM.

Fig. 3: Trajectories from different sampling distributions. Pedestrians and their future paths are in purple. The robot is at the red dot and the goal is the blue dot.



(a) $w_{\text{safe}} = 0$. (b) $w_{\text{safe}} = 0.5$. (c) $w_{\text{safe}} = 0.9$.

Fig. 4: Trajectories generated by different CBF reward weights using reward-guided CFM. Pedestrians and their future paths are in purple. The robot is at the red dot and the goal is the blue dot.

generation process was guided by the same reward functions and weights as CFM, but with a different set of safety reward weights $w_{\text{safe}} = [0.1, 0.2, 0.3, 0.4, 0.5]$. This adjustment was necessary because the diffusion model evaluates the reward function on noisy trajectories. The resulting noisy gradient information can cause overly conservative behavior, which the modified weights help to counteract.

Evaluation metrics. Each method is evaluated using the following metrics: **Collision**: Percentage of simulations that violate the collision radius. **Reaching**: Distance between the goal and the final point. **Smoothness**: Rate of change in control inputs over time. **Time**: Computation time required to compute the control input at each time step.

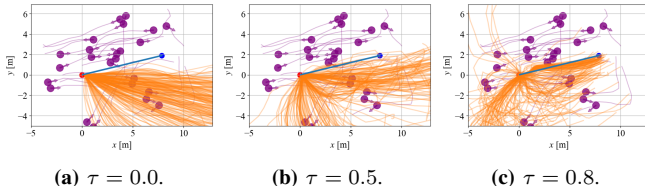
B. Qualitative results

We present some qualitative results of our method, highlighting its ability to capture multimodal sampling distributions and synthesize desirable robot trajectory plans.

Trajectory quality. The sampling distribution for each method is shown in Fig. 3. The CFM generates diverse trajectories heading downward, where the agent density is lower; the diffusion model generates trajectories more scattered throughout. The Gaussian distribution from standard MPPI does not incorporate environmental information, resulting in trajectories overlapping areas with higher agent density.

Diverse trajectories. Fig. 4 illustrates how various trajectories with varying conservativeness can be generated by changing the weight of CBF guidance w_{safe} . With smaller w_{safe} values, the trajectories move more directly toward the goal, while with larger weights, the trajectories avoid obstacles more drastically. Additionally, we see that the generated trajectories are *multimodal*, where trajectories tend to cluster around gaps in between the human agents.

CFM warm-starting. Fig. 5 illustrates the warm-start approach of CFM. It shows that reducing the noise applied to the previous optimal solution (i.e., higher τ) generates trajectories more similar to the previous trajectory. Stronger warm-starting may be beneficial when the environment does



(a) $\tau = 0.0$. (b) $\tau = 0.5$. (c) $\tau = 0.8$.

Fig. 5: Trajectories from CFM using warm-starts of varying strengths, based on previous optimal solution in blue. Pedestrians and their future paths are in purple. The robot is at the red dot and the goal is the blue dot.

TABLE I: Quantitative performance comparison of navigation algorithms for unicycle dynamics.

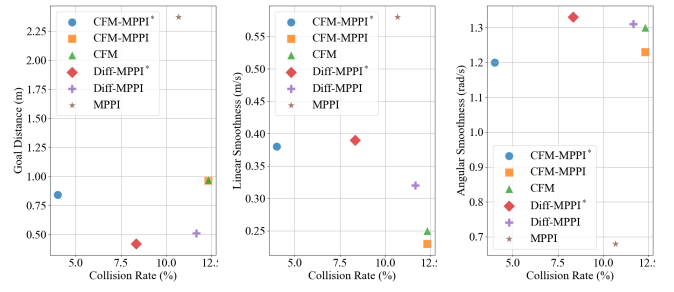
Method	Coll. (%) ↓	Reach. (m) ↓	Time (s) ↓
UCY Dataset			
MPPI	4.33	0.16±0.29	0.003
Diff-MPPI	0.67	0.23±0.07	0.085
Diff-MPPI*	0.00	0.20±0.06	0.091
CFM	0.33	0.06±0.01	0.066
CFM-MPPI	0.00	0.07±0.03	0.065
CFM-MPPI*	0.00	0.08±0.01	0.071
SDD Dataset			
MPPI	1.67	0.06±0.02	0.003
Diff-MPPI	2.33	0.26±0.09	0.085
Diff-MPPI*	0.67	0.20±0.10	0.091
CFM	0.00	0.05±0.00	0.066
CFM-MPPI	0.00	0.05±0.00	0.065
CFM-MPPI*	0.00	0.06±0.01	0.071
Simulated Crowd Environment with Social Force Model			
MPPI	24.67	1.89±5.13	0.003
Diff-MPPI	10.33	0.57±0.88	0.086
Diff-MPPI*	6.00	0.49±0.61	0.093
CFM	7.67	0.84±1.23	0.067
CFM-MPPI	8.00	0.79±1.18	0.066
CFM-MPPI*	2.33	0.72±1.09	0.073

not change rapidly and the previous solution is likely still desirable, and vice versa. In our current framework, the strength of warm start is fixed, but future work should explore methods to adjust this warm-start strength dynamically.

C. Quantitative results and key takeaways

Table I presents the metrics from evaluation on the test dataset and the SFM simulator, while Figure 6 shows the performance on the SFM simulator with noisy observations.

Takeaway 1. We observe that methods with CFM perform favorably than methods with diffusion. CFM methods (CFM, CFM-MPPI, CFM-MPPI*) demonstrate superior safety performance, while the goal-reaching method, although not always the best, still offers close-to-best performance. CFM methods also yield smoother outputs, despite mapping to unicycle dynamics. However, we note that safety and goal-reaching objectives can conflict with each other. For instance, to avoid collision, the robot may slow down or take a longer path, thus it is not able to reach the goal as closely within the allotted time. We also hypothesize that the reason why diffusion methods achieve lower safety performance is due to the evaluation of the reward function on noisy trajectories. While increasing the denoising steps can provide stronger safety guarantees, this increases computation times.



(a) Safety vs. goal. (b) Safety vs. linear (c) Safety vs. angular smooth.

Fig. 6: Performance comparison of each method evaluated on the SFM environment with noisy observations.

Takeaway 2. Mode selection improves robustness. In the SFM environment where agents are reactive and there is observation noise, we see that methods with mode selection perform noticeably better than their counterparts without mode selection. This highlights the benefit of additional refinement around promising candidates as opposed to refinement across diverse candidates. This observation motivates future work in investigating more sophisticated methods in selecting top candidates (e.g., considering diversity) to improve robustness further.

Takeaway 3. A learned sampling prior offers strictly better safety and task performance than an uninformed one. Aside from computation times, MPPI performs the worst in all settings, especially in the SFM environment where agents are reactive. While this is not a surprising result, the combination of takeaways 1 and 2 suggests that the quality of the priors and how they are utilized also play an important role in the performance and robustness of the approach.

Takeaway 4. CFM achieves a better trade-off between computational cost and performance than diffusion models. A key advantage of CFM is computational efficiency, which can generate controls in less than 0.1 seconds. For both CFM and diffusion models, the computational bottle neck is the reward calculation, which is performed at each guidance step. Since CFM requires fewer steps than diffusion models, it reduces the number of reward calculations. When we configured a diffusion model to be competitive with CFM in terms of speed, its performance on safety metrics degraded. While increasing the number of guided denoising steps to 20 improved the safety of Diff-MPPI*, its performance still did not match that of CFM-MPPI*, and its computation time doubled. Our observations show that CFM is more effective in generating higher quality trajectories within a much smaller computational budget.

VIII. CONCLUSION

We presented a planning framework integrating conditional flow matching (CFM) with sampling-based model predictive control (MPC), for multiagent dynamic environments. We develop a *reward-guided* CFM technique to generate multimodal informed priors for sampling-based MPC optimization while using MPC solutions to warm-start next CFM generation. Furthermore, to effectively leverage these multimodal priors, we introduced a mode-selective

MPPI that first identifies promising trajectory modes and then optimizes them in parallel to circumvent the common pitfall of averaging distinct paths into a suboptimal trajectory. We demonstrated the effectiveness of our system in various social navigation settings and show that our framework achieves favorable safety, goal achievement, and naturalness while maintaining real-time performance. For future work, we are considering dynamically adjusting the trade-off between mode exploration and optimization in response to previous solution quality and environmental challenges.

REFERENCES

- [1] A. Rudenko, L. Palmieri, M. Herman, K. M. Kitani, D. M. Gavrila, and K. O. Arras, “Human motion trajectory prediction: A survey,” *Int. Journal of Robotics Research*, vol. 39, no. 8, pp. 895–935, 2020.
- [2] K. Leung, E. Schmerling, M. Zhang, M. Chen, J. Talbot, J. C. Gerdes, and M. Pavone, “On Infusing Reachability-Based Safety Assurance within Planning Frameworks for Human-Robot Vehicle Interactions,” *Int. Journal of Robotics Research*, vol. 39, pp. 1326–1345, 2020.
- [3] E. Schmerling, K. Leung, W. Vollprecht, and M. Pavone, “Multimodal Probabilistic Model-Based Planning for Human-Robot Interaction,” in *Proc. IEEE Conf. on Robotics and Automation*, 2018.
- [4] H. Nishimura, B. Ivanovic, A. Gaidon, M. Pavone, and M. Schwager, “Risk-Sensitive Sequential Action Control with Multi-Modal Human Trajectory Forecasting for Safe Crowd-Robot Interaction,” in *IEEE/RSJ Int. Conf. on Intelligent Robots & Systems*, 2020.
- [5] M. Everett, Y. F. Chen, and J. P. How, “Motion Planning Among Dynamic, Decision-Making Agents with Deep Reinforcement Learning,” in *IEEE/RSJ Int. Conf. on Intelligent Robots & Systems*, 2018.
- [6] G. Williams, P. Drews, B. Goldfain, J. M. Rehg, and E. A. Theodorou, “Aggressive driving with model predictive path integral control,” in *Proc. IEEE Conf. on Robotics and Automation*, 2016.
- [7] D. P. Scharf, B. Açıkmese, D. Dueri, J. Benito, and J. Casoliva, “Implementation and experimental demonstration of onboard powered-descent guidance,” *AIAA Journal of Guidance, Control, and Dynamics*, vol. 40, no. 2, pp. 213–229, 2017.
- [8] C. Chi, S. Feng, Y. Du, Z. Xu, E. Cousineau, B. Burchfiel, and S. Song, “Diffusion Policy: Visuomotor Policy Learning via Action Diffusion,” in *Robotics: Science and Systems*, 2023.
- [9] B. Açıkmese and L. Blackmore, “Lossless convexification of a class of optimal control problems with non-convex control constraints,” *Automatica*, vol. 47, no. 2, pp. 341–347, 2011.
- [10] O. de Groot, B. Brito, L. Ferranti, D. Gavrila, and J. Alonso-Mora, “Scenario-Based Trajectory Optimization in Uncertain Dynamic Environments,” *IEEE Robotics and Automation Letters*, vol. 6, no. 3, pp. 5389–5396, 2021.
- [11] J. Sohl-Dickstein, E. Weiss, N. Maheswaranathan, and S. Ganguli, “Deep Unsupervised Learning using Nonequilibrium Thermodynamics,” in *Int. Conf. on Machine Learning*, 2015.
- [12] J. Ho, A. Jain, and P. Abbeel, “Denoising Diffusion Probabilistic Models,” in *Conf. on Neural Information Processing Systems*, 2020.
- [13] M. Janner, Y. Du, J. Tenenbaum, and S. Levine, “Planning with Diffusion for Flexible Behavior Synthesis,” in *Int. Conf. on Machine Learning*, 2022.
- [14] Y. Lipman, R. Chen, H. Ben-Hamu, M. Nickel, and M. Le, “Flow Matching for Generative Modeling,” in *Int. Conf. on Learning Representations*, 2023.
- [15] E. Chisari, N. Heppert, M. Argus, T. Welschehold, T. Brox, and A. Valada, “Learning robotic manipulation policies from point clouds with conditional flow matching,” in *Conf. on Robot Learning*, 2024.
- [16] S. Ye and M. Gombolay, “Efficient trajectory forecasting and generation with conditional flow matching,” in *IEEE/RSJ Int. Conf. on Intelligent Robots & Systems*, 2024.
- [17] J. Sacks and B. Boots, “Learning sampling distributions for model predictive control,” in *Conf. on Robot Learning*, 2023.
- [18] S. Banerjee, T. Lew, R. Bonalli, A. Alfaadhel, I. A. Alomar, H. M. Shageer, and M. Pavone, “Learning-based Warm-Starting for Fast Sequential Convex Programming and Trajectory Optimization,” in *IEEE Aerospace Conference*, 2020.
- [19] T. Guffanti, D. Gammelli, S. D’Amico, and M. Pavone, “Transformers for Trajectory Optimization with Application to Spacecraft Rendezvous,” in *IEEE Aerospace Conference*, 2024.
- [20] K. Honda, N. Akai, K. Suzuki, M. Aoki, H. Hosogaya, and H. Okuda, “Stein Variational Guided Model Predictive Path Integral Control: Proposal and Experiments with Fast Maneuvering Vehicles,” in *Proc. IEEE Conf. on Robotics and Automation*, 2023.
- [21] T. Power and D. Berenson, “Learning a Generalizable Trajectory Sampling Distribution for Model Predictive Control,” *IEEE Transactions on Robotics*, vol. 40, pp. 2111–2127, 2024.
- [22] A. Li and R. Beeson, “Aligning Diffusion Model with Problem Constraints for Trajectory Optimization,” *Available at <https://arxiv.org/abs/2504.00342>*, 2025.
- [23] E. Sharony, H. Yang, T. Che, M. Pavone, S. Mannor, and P. Karkus, “Learning multiple initial solutions to optimization problems,” *Available at <https://arxiv.org/abs/2411.02158>*, 2025.
- [24] E. Trevisan and J. Alonso-Mora, “Biased-MPPI: Informing Sampling-Based Model Predictive Control by Fusing Ancillary Controllers,” *IEEE Robotics and Automation Letters*, vol. 9, no. 6, pp. 5871–5878, 2024.
- [25] L. Jung, A. Estornell, and M. Everett, “Continuous Contingency Planning with MPPI within MPPI,” in *Learning for Dynamics & Control Conference*, 2025.
- [26] P. Kothari, S. Kreiss, and A. Alahi, “Human trajectory forecasting in crowds: A deep learning perspective,” *IEEE Transactions on Intelligent Transportation Systems*, vol. 23, no. 7, pp. 7386–7400, 2022.
- [27] W. Nie, A. Vahdat, and A. Anadkumar, “Controllable and Compositional Generation with Latent-Space Energy-Based Models,” in *Conf. on Neural Information Processing Systems*, 2021.
- [28] J. Ho and T. Salimans, “Classifier-Free Diffusion Guidance,” in *Conf. on Neural Information Processing Systems: Workshop on Deep Generative Models and Downstream Applications*, 2021.
- [29] J. Carvalho, A. Le, M. Baierl, D. Koert, and J. Peters, “Motion Planning Diffusion: Learning and Planning of Robot Motions with Diffusion Models,” in *IEEE/RSJ Int. Conf. on Intelligent Robots & Systems*, 2023.
- [30] Y. Meng and C. Fan, “Diverse Controllable Diffusion Policy With Signal Temporal Logic,” *IEEE Robotics and Automation Letters*, vol. 9, no. 10, pp. 8354–8361, 2024.
- [31] Z. Zhong, D. Rempe, D. Xu, Y. Chen, S. Veer, T. Che, B. Ray, and M. Pavone, “Guided Conditional Diffusion for Controllable Traffic Simulation,” in *Proc. IEEE Conf. on Robotics and Automation*, 2023.
- [32] W. Xiao, T. Wang, C. Gan, R. Hasani, M. Lechner, and D. Rus, “Safediffuser: Safe planning with diffusion probabilistic models,” in *Int. Conf. on Learning Representations*, 2025.
- [33] Q. Zheng, M. Le, N. Shaul, Y. Lipma, A. Grover, and R. T. Q. Chen, “Guided Flows for Generative Modeling and Decision Making,” *Available at <https://arxiv.org/abs/2311.13443>*, 2023.
- [34] R. Chen, Y. Rubanova, J. Bettencourt, and D. Duvenaud, “Neural ordinary differential equations,” in *Conf. on Neural Information Processing Systems*, 2018.
- [35] S. Levine, “Reinforcement Learning and Control as Probabilistic Inference: Tutorial and Review,” *Available at <https://arxiv.org/abs/1805.00909>*, 2018.
- [36] K. Mizuta and K. Leung, “CoBL-Diffusion: Diffusion-Based Conditional Robot Planning in Dynamic Environments Using Control Barrier and Lyapunov Functions,” in *IEEE/RSJ Int. Conf. on Intelligent Robots & Systems*, 2024.
- [37] A. D. Ames, S. Coogan, M. Egerstedt, G. Notomista, K. Sreenath, and P. Tabuada, “Control barrier functions: Theory and applications,” in *European Control Conference*, 2019.
- [38] J. Geldenbott and K. Leung, “Legible and Proactive Robot Planning for Prosocial Human-Robot Interactions,” in *Proc. IEEE Conf. on Robotics and Automation*, 2024.
- [39] S. Pellegrini, A. Ess, Schindler, and L. Gool, “You’ll Never Walk Alone: Modeling Social Behavior for Multi-Target Tracking,” in *IEEE Int. Conf. on Computer Vision*, 2009.
- [40] A. Lerner, Y. Chrysanthou, and D. Lischinski, “Crowds by Example,” *Computer Graphics Forum*, vol. 26, no. 3, pp. 655–664, 2007.
- [41] A. Robicquet, A. Sadeghian, A. Alahi, and S. Savarese, “Learning social etiquette: Human trajectory prediction in crowded scenes,” in *European Conf. on Computer Vision*, 2016.
- [42] D. Helbing and P. Molnár, “Social force model for pedestrian dynamics,” *Physical Review E*, vol. 51, no. 5, pp. 4282–4286, 1995.
- [43] A. Vaswani, N. Shazeer, N. Parmar, J. Uszkoreit, L. Jones, A. N. Gomez, L. Kaiser, and I. Polosukhin, “Attention is All You Need,” in *Conf. on Neural Information Processing Systems*, 2017.